ACS OMEGA

Open Access

http://pubs.acs.org/journal/acsodf

Article

Reactivity and Dissolution Characteristics of Naturally Altered Basalt in CO_2-Rich Brine: Implications for CO_2 Mineralization

Published as part of ACS Omega virtual special issue "CO2 Geostorage".

Jiajie Wang,* Masahiko Yagi, Tetsuya Tamagawa, Hitomi Hirano, and Noriaki Watanabe*

Cite This: *ACS Omega* 2024, 9, 4429−4438

Read Online

ACCESS | Metrics & More | Article Recommendations

ABSTRACT: Hydrothermally altered basaltic rocks are widely distributed and more accessible than fresh basaltic rocks, making them attractive feedstocks for permanent CO_2 storage through mineralization. This study investigates the reactivity and dissolution behaviors of altered basalt during the reaction with CO_2-rich fluids and compares it with unaltered basalt through batch hydrothermal experiments using a brine that simulates reservoir conditions with 5 MPa CO_2 gas at 100 °C. When using basalt powders to evaluate reactivity, results show that although the leaching rates of elements (Mg, Al, Si, K, and Fe) from altered basalt were generally an order of magnitude lower than those from unaltered basalt in a CO_2-saturated acidic environment, similar elemental leaching behavior was observed for the two basalt samples, with Ca and Mg having the highest leaching rates. However, in a more realistic environment simulated by block experiments, different leaching behaviors were observed. When the CO_2-rich fluid reacts with altered basalt, rapid and preferential dissolution of smectite occurs, providing a significant amount of Mg to the solution, while Ca dissolution lags. This implies that when altered basalt is utilized for CO_2 mineralization, the carbonation step may differ from that of fresh basalt, with predominant Mg carbonation followed by Ca carbonation. This rapid dissolution of Mg suggests that altered basalt is a promising feedstock for CO_2 mineralization. This study provides theoretical support for developing technologies to utilize altered basalt for carbon storage.

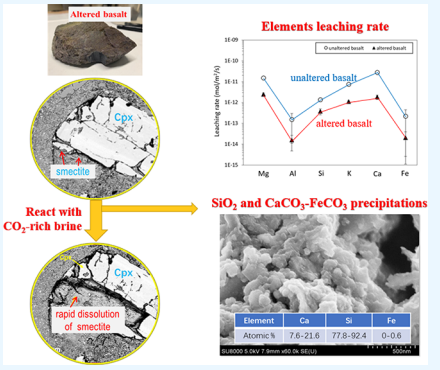

1. INTRODUCTION

Mineral carbonation involves the reaction of carbon dioxide (CO_2) with metal oxide-bearing minerals and rocks to form insoluble carbonate minerals, with calcium (Ca), magnesium (Mg), and iron (Fe) being the most attractive metals.[1−3] In recent years, the enhancement of the mineral carbonation process has attracted attention as a potential approach for mitigating atmospheric CO_2 levels and preventing the impacts of climate change.

Basaltic rocks, which are widely distributed, are considered particularly promising candidates owing to their high reactivity and significant content of Ca, Mg, and Fe oxides, which together constitute approximately 25% of their weight.[4,5] The theoretical storage capacity of the submarine basalt has been estimated to range from 100,000 to 250,000 $GtCO_2$,[6] which is orders of magnitude larger than the amount of CO_2 that must be removed to limit global warming to 1.5 °C.[7] Numerous studies and a few field projects have assessed the feasibility of CO_2 storage in basalt,[8−10] with promising results reported in the CarbFix project in southwest Iceland.[11] In this project, the injected CO_2 was predominantly converted into stable carbonate minerals within two years.

The basaltic rocks in CarbFix were relatively fresh and composed mainly of pyroxenes, plagioclase, and olivine,[12,13] which are known to be highly reactive minerals.[14] However, fresh basaltic rocks are restricted to active volcanic systems and rift zones, and most widespread basaltic rocks have undergone varying degrees of alteration through reactions with hydrothermal fluids.[15,16] In Japan, many oil and gas field reservoirs located on the Sea of Japan side of the Northeast Japan Arc are associated with basaltic rocks that erupted and were deposited on the seafloor during the Early to Middle Miocene and Late Miocene to Pliocene periods.[17] These reservoirs have undergone natural alteration, diagenesis, and hydrothermal activities under high geothermal gradients.[18,19] Although the use of existing wells in oil and gas fields for CO_2 storage is both technically and economically advantageous, the feasibility and effectiveness of using such altered basaltic formations for CO_2 mineralization remain uncertain. Therefore, understanding the

Received: September 10, 2023
Revised: November 27, 2023
Accepted: November 29, 2023
Published: January 17, 2024

https://doi.org/10.1021/acsomega.3c06899
ACS Omega 2024, 9, 4429−4438

reactivity of altered basalt is crucial for the development of effective strategies for CO_2 mineralization using basalt.

Hydrothermal alteration of basaltic rocks causes extensive changes in their mineralogy, chemical composition, and porosity. In the case of seawater-induced basalt alteration, the predominant mineralogical transformations were albite−actinolite−chlorite−epidote assemblages.[20] These secondary minerals (e.g., clay minerals) are typically 1 to 4 orders of magnitude lower than those of plagioclase and pyroxenes,[21−24] reducing the reactivity of basalt.[25] Meanwhile, the thin and flaky structure of clay minerals in altered basalt offers a large surface area for reactions. Clay minerals have up to 150 times the specific surface area (SSA) of pyroxene and olivine;[26] for instance, the SSA of smectite can reach 750 m^2/g.[27] Basaltic rocks also undergo chemical changes during alteration, with a higher MgO and lower CaO content than fresh basaltic rocks.[28] Ca is an important element in mineralizing dissolved CO_2,[29] and calcite is an essential product of CO_2 mineralization at the CarbFix project site.[30] Hence, it is necessary to determine whether altered basalt containing clay minerals is an effective cation source for CO_2 storage and how changes in basaltic chemical compositions alter elemental dissolution behaviors.

According to basalt dissolution experiments carried out at pH 3 and 120 °C using a fluid containing HCl and NaCl, Delerce et al.[15] suggested that the dissolution of altered basalt is not as efficient as that of unaltered basalt; however, the reactivity is independent of the degree of alteration in basalt. Liu et al.[13] also hypothesized that the CO_2 mineralization efficiency is lower in altered basalt than in unaltered basalt based on modeling. Nevertheless, Shao et al.[31] and recently Liu et al.[32] suggested that clay minerals, including smectite, chlorite, and phlogopite, are also important minerals contributing to CO_2 storage in basaltic reservoirs.

To evaluate the feasibility of using altered basaltic reservoirs for CO_2 mineralization, this study investigated the reactivity and dissolution behaviors of altered basalt through batch dissolution experiments conducted at 100 °C and 5 MPa CO_2 gas and compared it with unaltered basalt. Both basalt samples were obtained from an oilfield located on the Sea of Japan side of the Northeast Japan Arc. An artificial brine that mimics the real geofluid in the sampling site was used instead of water in the experiments. The effect of brine may be crucial in the mineralization process as the NaCl in brine and the associated alkalinity may significantly impact mineral dissolution and carbonation.[33−35] Therefore, the use of brine that mimics the geofluid of a geological setting is important for understanding the reactivity of basalt in a target CO_2 storage reservoir. The findings of this study on altered basalts are expected to contribute to the development of effective CO_2 mineralization strategies using basaltic rocks both underground and on the ground.

2. MATERIALS AND METHODS

2.1. Rock Samples and Brine Preparation. Most oil and gas fields in Japan occur in coastal areas of the Sea of Japan, as shown in Figure 1, as suggested by Huzioka.[36] Their reservoirs typically comprise erupted volcanic rocks and clastic rocks deposited on the seafloor during the Early to Middle Miocene and Late Miocene to Pliocene periods. However, the reservoirs have been altered, with clay minerals formed by diagenesis and hydrothermal activity associated with a high geothermal gradient (inferred at >15 °C/100 m by Yagi[18]) in a back-arc rift setting. The basalt samples in this study were sampled from a gas reservoir in an oilfield in Niigata on the Sea of Japan side of the Northeast Japan Arc, at a depth of 1000 m, as shown in Figure 1. The dissolution samples were categorized as altered and unaltered basalts based on the presence or absence of clay minerals in the rock detected via microscopic observation of thin section samples.

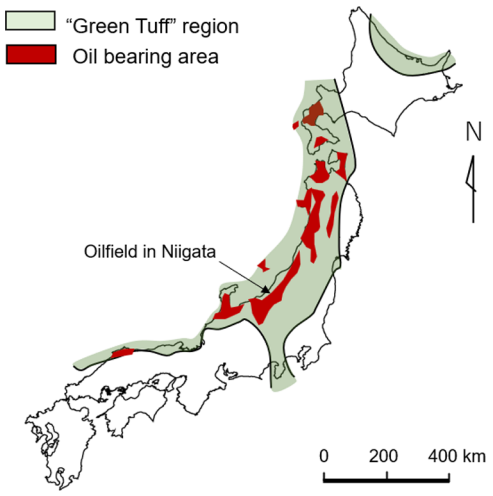

Figure 1. Distribution of "Green Tuff" stage basalts, oil-bearing area, and the location of the basaltic rock sampling site.

The bulk chemical compositions of these rocks were determined by using X-ray fluorescence spectrometry (XRF; Rigaku, ZSX Primus IV). The powder basalt was measured for its mineral composition using X-ray diffraction (XRD; Multiflex, Rigaku, Japan) with Cu Kα radiation (λ = 1.54 Å) operated at 40 kV and 20 mA and with a 2θ step size of 0.02° from 5° to 50°. The mineralogical characteristics were determined using an electron probe microanalyzer (EPMA; Jeol JXA-8200). Quantitative and elemental mapping analyses of the major minerals were conducted at an accelerating voltage of 15 kV and beam currents of 12 and 120 nA, respectively. ImageJ software was employed to obtain the area fractions of the mineral assemblages from the backscattered electron (BSE) images or elemental maps of each sample obtained from the EPMA. Each mineral was quantitatively analyzed at 5−10 points to obtain the average chemical composition.

Both powders and blocks of the basalt samples were used for dissolution experiments (Figure 2a). To prepare the basalt powders, the rocks were ground and sieved to obtain the <150 μm-sized fractions. To ensure that the mineral composition of the powder samples was consistent with the original rocks, pretreatment for fine particle removal, such as ultrasonic treatment, was not applied in this study. The particle size distributions of the rock powders were analyzed using a particle size analyzer (Mastersizer 3000, Malvern Panalytical Ltd., UK), and the results are shown in Figure 2b. The specific surface areas (SSA) of the basalt powders were examined by the N_2-BET method using an Autosorb-iQ_ ASIQM0000-3 (Quantachrome Instruments, Florida, USA). For unaltered basalt, measurement data in the relative pressure (P/P_0) range of 0.10 to 0.30 were used, while that for unaltered basalt was 0.07−0.13. The unaltered and altered basalt powders exhibited SSA values of 2.2 and 23.7 m^2/g, respectively. For the block experiments, basalt rocks were cut into approximately 18 × 5 × 5 mm rectangular cuboids (Figure 2a).

https://doi.org/10.1021/acsomega.3c06899
ACS Omega 2024, 9, 4429−4438

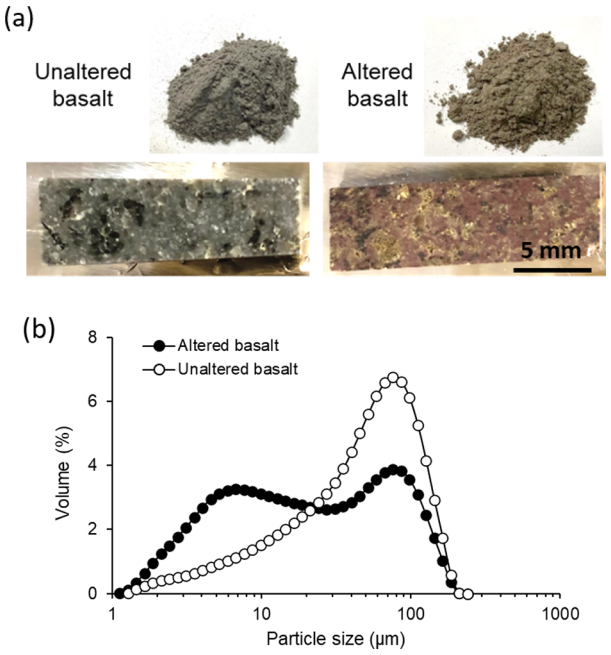

Figure 2. (a) Pictures of powder and block samples of unaltered and altered basalt and (b) particle size distributions of the powder samples.

To simulate a realistic environmental condition for the reaction, a brine solution was prepared based on the results of field groundwater monitoring. This solution mainly contained Na^+, Ca^{2+}, Cl^-, HCO_3^-, and SO_4^{2-} from the dissolution of solid NaCl (purity > 99.5%), sodium bicarbonate ($NaHCO_3$; purity > 99.0%), calcium chloride ($CaCl_2$; purity > 95.0%), and sulfuric acid (H_2SO_4; purity > 96.0%) in Milli-Q water purchased from Kanto Chemical, Japan. Specifically, 3.04 g of NaCl, 0.31 g of $NaHCO_3$, and 0.27 g of $CaCl_2$ powders were dissolved in 1 L of Milli-Q water, and the pH was adjusted to 6.6 by adding a small volume of a H_2SO_4 solution. The elemental compositions were then analyzed by inductively coupled plasma-optical emission spectrometry (ICP-OES; Agilent 5100), as shown in Table 1.

Table 1. Chemical Compositions and pH of Brine Prepared for the Experiments

	mg/L
Na^+	1281
Ca^{2+}	96
Cl^-	2016
HCO_3^-	226
SO_4^{2-}	120
pH	6.6

2.2. Experimental Methods. The batch dissolution experiments were conducted under conditions that reflected the likely reservoir conditions of the research area (i.e., 100 °C) using a high-temperature and high-pressure closed-batch autoclave made of Hastelloy-C with a 170 mL volume. A comprehensive description of the autoclave is provided in our previous study.[14] The maximum tolerable temperature and pressure of the autoclave were 300 °C and 20 MPa, respectively. Injecting CO_2 gas into the reactor decreased the solution pH and promoted mineral dissolution. Considering that the solution pH decreases with increasing CO_2 pressure yet remains relatively stable when the CO_2 pressure exceeds 5 MPa at <100 °C, 5 MPa CO_2 was applied for mineral dissolution.

In a typical run, a 100 mL suspension containing 5 ± 0.01 g of basalt powder and brine with a water/rock weight ratio of 20 was charged into the autoclave vessel, which was then subjected to continuous stirring. This water/rock ratio was decided based on previous similar studies on basalt alteration,[8,37] including our previous study conducted at 200−300 °C, in which significant dissolution and carbonation of basalt powders were observed. Although this water/rock ratio may be much higher than that in subsurface environments, this difference is not expected to significantly impact the evaluation of rock reactivity and dissolution behaviors. The reactor was then sealed and purged with N_2 gas through the sampling tube to facilitate O_2 removal from the solution and the upper headspace. After 5 min, the air outlet was closed, and CO_2 gas was injected through the same sampling tube to reach the desired pressure of 5.0 MPa. Once the temperature was set to 100 °C, it took approximately 10 min for the reactor temperature to stabilize. In this experimental environment, the solubility of CO_2 was calculated to be approximately 2×10^4 mg/L.[38] The reactions were allowed to proceed for 360 h. This reaction time was slightly longer than that of our previous study, which achieved basalt dissolution and carbonation in 120−240 h using a relatively high temperature (200 °C).[8] After that, the reactor temperature was lowered to below 40 °C by using cool water, which took around 10 min. The pH of the reacted suspension was measured at ambient temperature. The suspension was then filtered through a 0.45 μm membrane to separate fluid and solid samples; the latter was dried at 50 °C for 24 h in an oven before further analysis. Each powder experiment was performed in duplicate.

For the block experiments, one face of each block sample was wet-polished by using a diamond slurry before the reaction and examined by using the EPMA to confirm the mineral assemblages and compositions. The blocks were then added to 100 mL of the brine solution for the reaction with a rock-to-water ratio of approximately 130 g/L, relatively lower than the powder experiments. No stirring was applied during the reaction period of 360 h to ensure that the rock samples were not damaged by physical actions. After cooling the system and obtaining the block samples, they were again analyzed by using the EPMA to evaluate the changes in the mineral surface.

2.3. Reactive Sample Analysis and Calculation. All liquid samples collected after the reactions were analyzed for pH at room temperature (approximately 20 °C) and by ICP-OES to quantify the target elements (Na, Mg, Al, Si, K, Ca, and Fe). Each fluid sample was measured three times to show good reproducibility within a margin of error of 3%. The mineral composition of the powder basalt samples before and after reactions was measured by using XRD, and the surface morphologies of the minerals were observed by scanning electron microscopy (SEM; SU-8000, Hitachi, Japan). Fourier transform infrared (FTIR, PerkinElmer, Japan) analyses of rock samples were performed to ascertain the generation of carbonates. To assess the reactivity of the rocks, the average element leaching rates in mol/m^2/s over the reaction time were calculated by dividing elemental concentrations in the reacted fluids with the rock dosage for the experiment (50 g/L), SSA of the initial rocks, and reaction time (360 h).

https://doi.org/10.1021/acsomega.3c06899
ACS Omega 2024, 9, 4429−4438

3. RESULTS AND DISCUSSION

3.1. Characterization of Basalt Samples. The bulk chemical compositions of basalt samples were determined by using XRF; the results are presented in Table 2. Altered basalt exhibited different compositions from the unaltered basalt, with relatively higher Mg and Fe contents and a lower Ca content. The mineral assemblages of altered and unaltered basalt samples were measured with the EPMA (Table 3). The mineral assemblages of unaltered basalt included plagioclase ($Ca_{0.56}Na_{0.41}K_{0.03}Al_{1.6}Si_{2.4}O_8$), clinopyroxene ($(Ca_{0.9}Mg_{0.1})(Mg_{0.7}Fe_{0.3})Si_2O_6$), orthopyroxene ($(Mg_{1.3}Fe_{0.7})Si_2O_6$), groundmass, Fe−Ti oxides, and small amounts of olivine and illite. In contrast, altered basalt comprised plagioclase ($Ca_{0.76}Na_{0.23}K_{0.01}Al_{1.7}Si_{2.3}O_8$), clinopyroxene ($(Ca_{0.9}Mg_{0.1})(Mg_{0.7}Fe_{0.3})Si_2O_6$), smectite, groundmass, and Fe−Ti oxides. Notably, in the core area of the plagioclase particles, the Ca content was relatively high, while the Na content was low compared to that in the rim area. Moreover, the groundmass of the unaltered and altered basalt contained small K-feldspar particles. Additionally, the estimated fraction of smectite was higher than the true value due to the large space contained inside the mineral caused by its typical thin and flaky structure.

Table 2. Bulk Chemical Composition of Basalt Samples Determined by X-ray Fluorescence Spectrometry (XRF) (Mass %)

	unaltered basalt	altered basalt
SiO_2	54.75	55.11
TiO_2	0.46	0.70
Al_2O_3	13.65	13.25
Fe_2O_3	4.58	8.44
MnO	0.14	0.06
MgO	2.24	9.38
CaO	6.48	5.64
Na_2O	2.69	2.31
P_2O_5	0.22	0.17
K_2O	2.28	2.17
LOI	8.80	3.80
Total	96.30	101.03

3.2. Reactivity of Altered Basalt. The average leached concentrations of elements in the fluids resulting from the reaction of the unaltered and altered basalt powders with brine in a CO_2-rich environment for 360 h are presented in Figure 3.

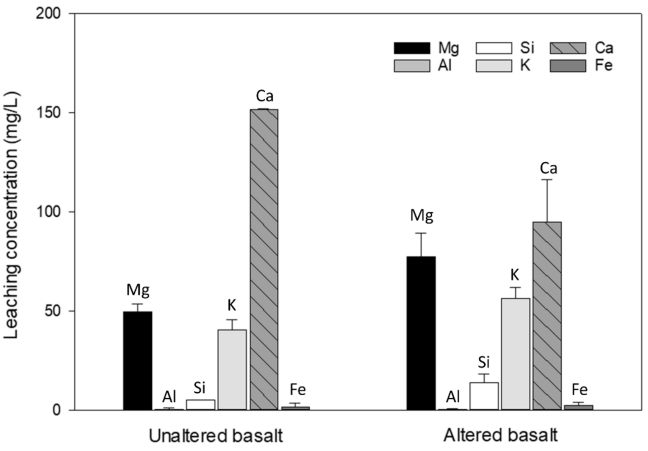

Figure 3. Element leaching concentrations after reacting unaltered and altered basalt powders in brine with 5 MPa CO_2 gas at 100 °C for 360 h. Ca concentrations were obtained by subtracting the initial concentration of 96.0 mg/L from measured values.

The Ca concentrations shown in the figure were obtained by subtracting the initial concentration of 96.0 mg/L (in initial brine) from the measured values, while the Mg, Si, Al, K, and Fe concentrations were used as measured.

Although the elemental contents of the altered and unaltered basalt samples differed (i.e., altered: Fe > Mg > Ca; unaltered: Ca > Fe > Mg), similar trends in elemental leaching were observed, with the highest leaching levels observed for Ca and Mg followed by K and Si, while Al and Fe were leached at 2 orders of magnitude less than Mg and Ca. In the dissolution experiment using altered basalt, the Ca concentration increased from the initial 96.0 to 190.7 mg/L in 360 h, with 94.7 mg/L of Ca leached; meanwhile, 77.2 mg/L Mg and 13.7 mg/L Si were leached from altered basalt. Notably, even though the initial rock samples contained a comparable amount of Fe relative to Ca and Mg, the leaching concentrations of Fe from altered and unaltered basalts were unexpectedly below 5.0 mg/

Table 3. Mineral Assemblages and Chemical Composition of the Main Minerals of Basalt Samples Ddetermined by an Electron Probe Microanalyzer (EPMA)

			average composition (mass %)										
sample	mineral	[a]fraction (%)	Na_2O	SiO_2	FeO	K_2O	TiO_2	Al_2O_3	MgO	MnO	Cl	CaO	total
unaltered basalt	plagioclase	29.2	4.90	53.73	0.44	0.43	0.05	29.11	0.07	n.d.	n.d.	12.01	100.75
	clinopyroxene	13.5	0.38	51.35	8.65	n.d.	0.42	1.61	13.09	0.48	n.d.	21.58	97.60
	orthopyroxene		0.02	52.08	19.18	n.d.	0.16	1.00	22.60	0.63	n.d.	1.15	96.85
	Fe−Ti oxides	2.5	n.d.	0.08	79.00	n.d.	9.80	2.40	1.50	0.70	n.d.	1.40	93.40
	[b]groundmass	54.8	0.38	51.35	8.65	3.00	0.43	1.61	13.10	0.48	n.d.	21.58	100.60
	olivine		not measured										
	illite		not measured										
altered basalt	plagioclase	29.3	2.73	49.70	0.66	0.23	0.02	32.35	0.08	0.06	n.d.	15.62	101.45
	smectite	24.5	n.d.	47.37	12.00	0.04	n.d.	4.16	17.40	0.04	n.d.	2.22	83.25
	clinopyroxene	8.6	0.28	51.09	7.68	n.d.	0.53	3.57	15.40	0.24	n.d.	21.37	100.17
	Fe−Ti oxides	2.7	n.d.	n.d.	77.87	n.d.	6.52	1.35	0.92	0.65	n.d.	0.10	87.41
	[b]groundmass	34.9	1.60	66.51	0.33	10.16	0.05	17.33	0.15	n.d.	n.d.	0.43	96.56

[a]Mineral fractions were determined based on the area of the mineral assemblages, excluding pores. [b]Chemical composition of K-feldspar in the groundmass was not determined.

https://doi.org/10.1021/acsomega.3c06899
ACS Omega 2024, 9, 4429−4438

L. This may be due to the reprecipitation of Fe-bearing minerals. The pH values of the reacted solutions at room temperature were 7.5 and 6.8 for the altered and unaltered basalt, respectively. This was considered the result of silicate dissolution (pH increase) and CO_2 dissolution (pH decrease). However, these pH values do not represent the true reaction conditions, as the calculated in situ pH value at 100 °C and 5 MPa CO_2 was <3.5.

The average element leaching rate in mol/m^2/s during the first 360 h with the CO_2-rich fluid was calculated and is summarized in Figure 4. Although no substantial difference in

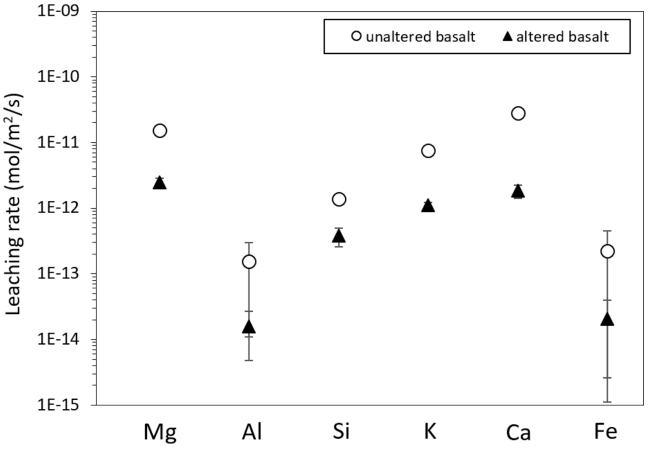

Figure 4. Leaching rates of elements (mol/m^2/s) from altered and unaltered basalt powders when reacting with brine at 5 MPa CO_2 gas and 100 °C in 360 h.

element concentrations was observed between the two types of basalt, as shown in Figure 3, owing to the relatively larger SSA of the altered basalt powders (23.7 m^2/g) than unaltered basalt powders (2.2 m^2/g), the rate of all elements leached from the altered basalt was generally an order of magnitude lower than those from the unaltered basalt. For example, 1.8×10^{-12} and 2.8×10^{-11} mol/m^2/s of Ca were leached from the altered and unaltered basalt, respectively. Considering that the compositions of Ca-bearing clinopyroxene and plagioclase are the same in both basalt samples, the higher Ca leaching rate from unaltered basalt may be attributed to groundmass dissolution. Notably, the leaching rates of Si and other metal cations were generally lower from unaltered basalt than previously reported.[15,24,39] For instance, the Si leaching rate was 1.4×10^{-12} mol/m^2/s in this study, while that reported by Rinder and von Hagke[39] was $0.7-2.1 \times 10^{-11}$ mol/m^2/s, implying a negative effect of brine on basalt dissolution. However, this leaching rate calculation is a simple assessment of rock reactivity and does not represent the actual kinetic dissolution process. Additional studies are warranted to assess the kinetics of altered basalt dissolution.

3.3. Mineralogy Characterization. The XRD patterns of the unaltered and altered basalt powders before and after the reactions are compared in Figure 5. In the case of the unaltered basalt powder, no noticeable changes were made to the mineral composition after dissolution. Conversely, for altered basalt, a marked decrease in the intensity of the smectite peak at 5.9° was observed,[40] suggesting a selective dissolution of smectite. Additionally, the overlapping peak belonging to plagioclase and pyroxenes at 27.8° decreased significantly, whereas the peaks for plagioclase alone, such as at 22.0°, decreased to a lesser

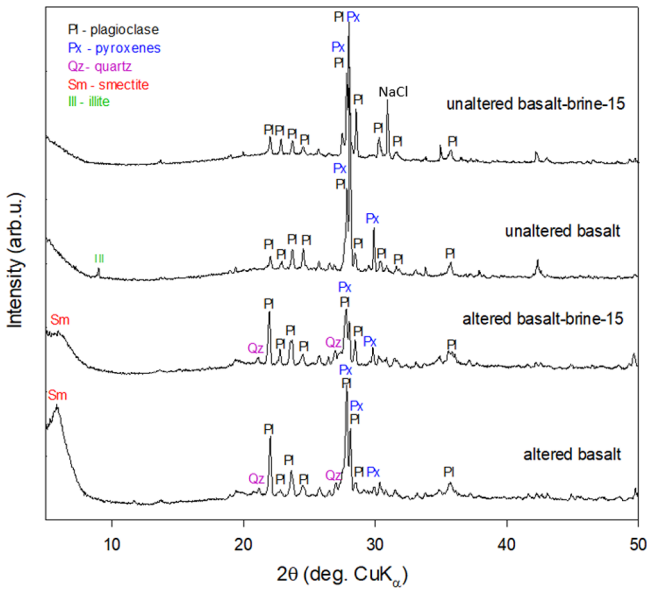

Figure 5. X-ray diffraction (XRD) patterns of basalt powders before and after reacting with brine at 5 MPa CO_2 gas and 100 °C for 360 h.

extent, suggesting a preferred dissolution of pyroxene over plagioclase. Based on the above XRD analysis results, it can be inferred that smectite and probably clinopyroxene in altered basalt have relatively higher reactivities, and their dissolution has contributed the majority of the Mg and Ca in solution, respectively (Figure 3). Based on the mineral compositions measured by the EPMA (shown in Table 3), the Mg/Ca weight ratios of smectite and clinopyroxene were 8.3 and 0.6, respectively; therefore, it can be inferred that most of the Ca in the solution was leached mainly from clinopyroxene, while Mg was from both smectite and clinopyroxene.

SEM observations revealed that unlike unaltered basalt powders that displayed a fresh surface (Figure 6a), most of the altered basalt powders were covered with smectite before the reaction (Figure 6b). However, after a 360 h reaction period in the brine and CO_2-rich environment, the majority of the smectite had dissolved, exposing the surfaces of other minerals, such as pyroxenes (Figure 6c). As a result, many small particles consisting mainly of Si and small amounts of Ca and Fe were observed on the surface previously occupied by smectite (Figure 6d), indicating the precipitation of amorphous SiO_2 and some Ca-bearing minerals from the dissolution of smectite and pyroxenes. By comparing the FTIR spectroscopy measurement results of the initially altered basalt with those after the dissolution experiment (Figure 7), a new peak was observed at 1445 cm^{-1}, inferring the presence of CO_3 according to Rodriguez-Blanco et al.[41] and Köck et al.[42] This observation, together with SEM-EDX results, suggests a coprecipitation of Ca−Fe carbonates with amorphous SiO_2. Kellermeier et al.[43] proposed the possibility of incorporating amorphous calcium carbonate (ACC) into the amorphous SiO_2 aggregates due to a local decrease in pH near the surface of ACC during its generation, although generally, the conditions for carbonate formation have not yet been reached.

3.4. Dissolution Behaviors of Block Basalt Samples. To understand the process of basalt dissolution upon CO_2 injection into the basaltic reservoir, block basalt samples (1.8 cm × 0.5 cm × 0.5 cm), which remained in the original size of the containing minerals, were also reacted with 100 mL of

https://doi.org/10.1021/acsomega.3c06899
ACS Omega 2024, 9, 4429−4438

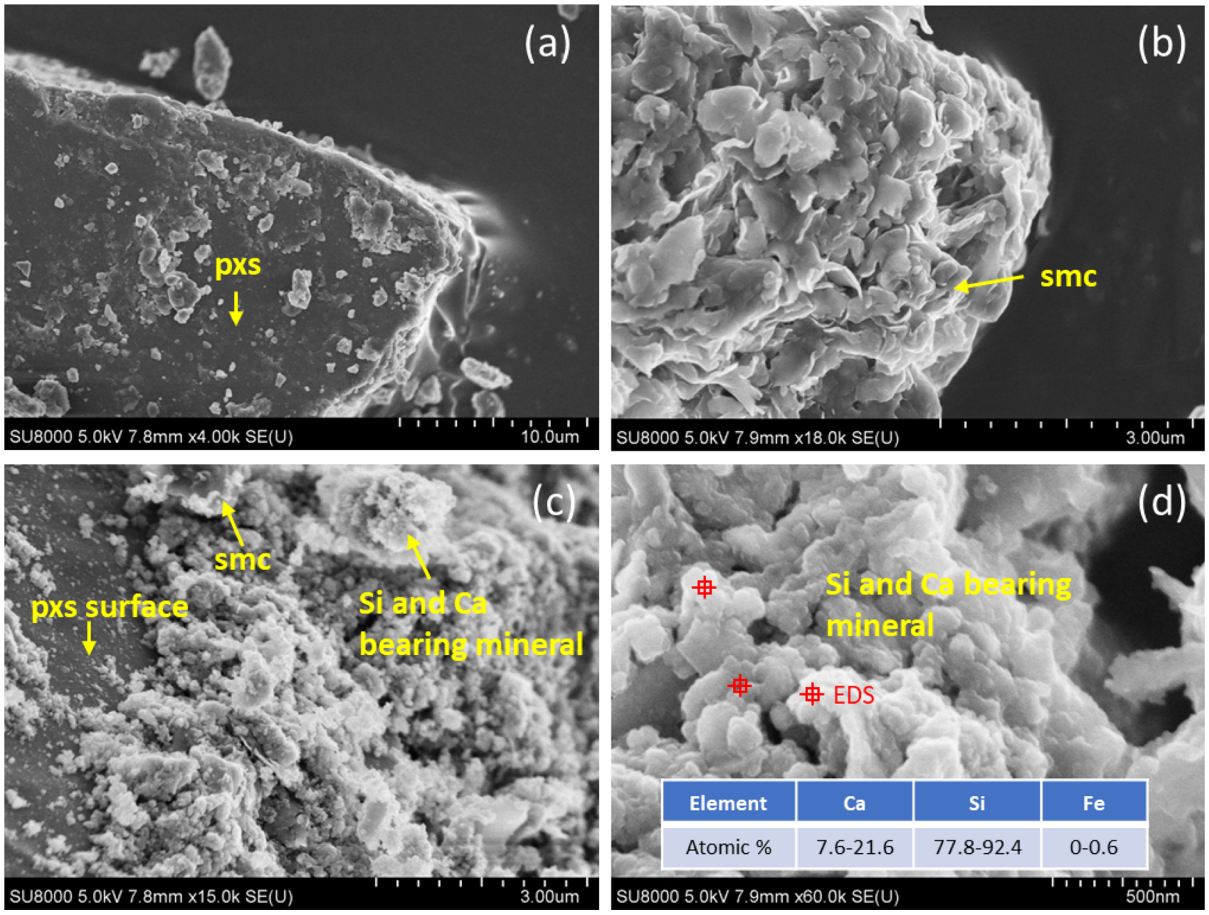

Figure 6. Scanning electron microscopy (SEM) images of (a) unaltered basalt and (b) altered basalt powders before reactions and (c,d) altered basalt powder after reacting with brine at 5 MPa CO_2 gas and 100 °C for 360 h; smc: smectite; pxs: pyroxenes.

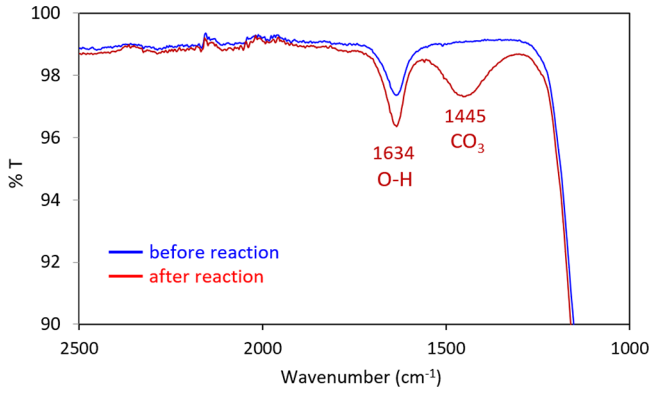

Figure 7. Fourier transform infrared (FTIR) spectra of altered basalt powder before and after reacting with brine at 5 MPa CO_2 gas and 100 °C for 360 h.

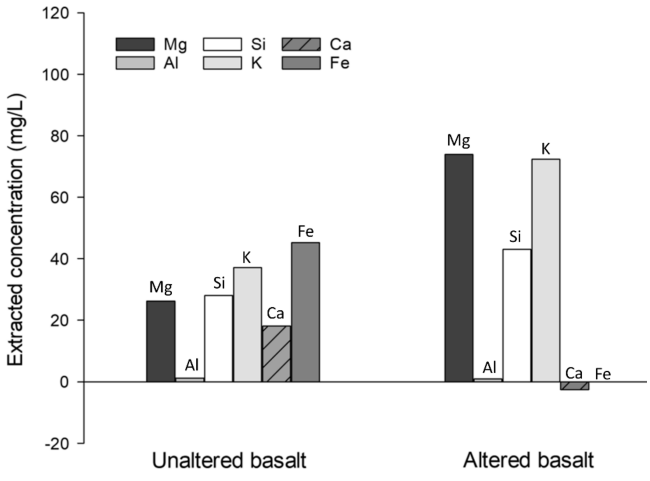

Figure 8. Changes in the chemical compositions of the fluid after reacting with altered and unaltered basalt block samples in brine with 5 MPa CO_2 gas at 100 °C for 360 h. Ca concentrations were obtained by subtracting the initial concentration of 96.0 mg/L from measured values.

brine at 5 MPa CO_2 and 100 °C. The chemical compositions of fluids obtained after a 360 h reaction are shown in Figure 8.

From both altered and unaltered basalts, less Ca than Mg was leached, which is inconsistent with the reactivity evaluation results in the powder experiments (Figure 4). In block-altered basalt experiments, the negligible change in Ca concentration suggests that clinopyroxene dissolved slowly, while the negative value is considered a measurement error. The difference between powder and block experimental results suggests that although clinopyroxene is a potential reactive Ca source in altered basalt, it may be less susceptible to dissolution in the basaltic reservoir due to the relatively larger grain size that resulted in a small contact area for reactions. To efficiently use Ca in altered basalt for CO_2 storage, rock fracturing or crushing techniques must be considered. Notably, different water−rock ratios in the powder and block experiments may have also contributed to the different element leaching results.

https://doi.org/10.1021/acsomega.3c06899
ACS Omega 2024, 9, 4429−4438

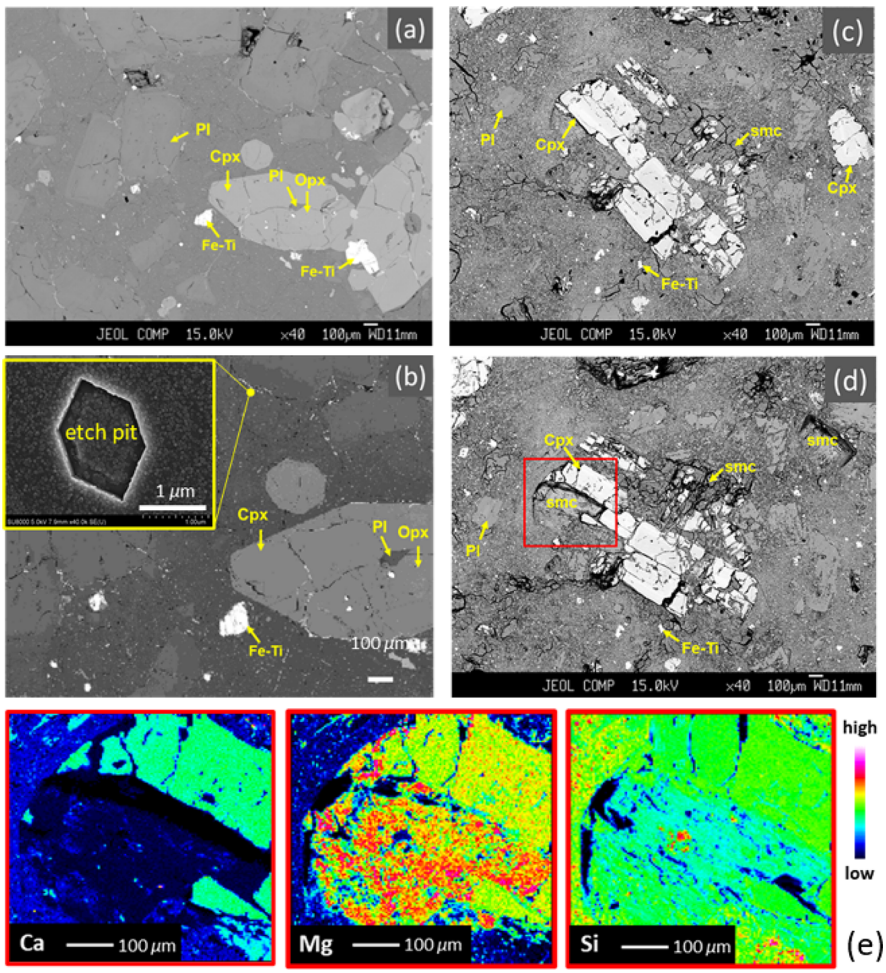

Figure 9. Results of the electron probe microanalyzer (EPMA) and scanning electron microscopy (SEM) of unaltered basalt block samples (a) before and (b) after the reaction and the altered basalt block (c) before and (d) after the reaction; (e) mapping results of Ca, Mg, and Si for the area shown in the red box in (d).

Meanwhile, the Mg concentration from altered basalt was 3-fold higher than that of unaltered basalt, suggesting that the leaching of Mg from altered basalt, especially from smectite dissolution, can occur rapidly in the basaltic reservoir. Dissolution of altered basalts yields higher concentrations of Si, implying that silicate minerals in altered basalts are not only as reactive as those in unaltered basalts, as illustrated in Figure 4, but also more susceptible to reaction by CO_2-rich solutions. The Fe concentration was higher in the block unaltered basalt experiment than in the powder experiment. This may be related to the lower Ca concentration in the block and the absence of carbonate formation, which can incorporate Fe.

Figure 9a,b shows SEM and EPMA observations of the same area in the unaltered basalt sample before and after the reaction. Although the mineral assemblages were not significantly changed according to EPMA measurements, SEM revealed the presence of numerous etch pits with a hexagonal shape and a size less than 2 μm among the groundmass (Figure 9b). These etch pits are assigned to olivine because they resemble the olivine crystal structure. The rapid dissolution of small olivine particles in unaltered basalt contributed to the Mg in solution, a process that can be considered as the initial step of unaltered basalt dissolution after CO_2 injection.

The morphological changes in the altered basalt block after dissolution can be observed by comparing Figure 9b and d. Several areas exhibited substantial dissolution of smectite, and some clinopyroxene pieces disappeared, as highlighted by the red box on the left side of Figure 9d. On examining the solution, a negligible increase in Ca concentration was observed, implying that clinopyroxene dropped from the surface rather than dissolved. Although the reactivity of Ca-bearing clinopyroxene is not low, as indicated by powder experiments, the leaching of Ca from block basalt proceeds at a sluggish rate due to the larger particle size of Ca-bearing clinopyroxene in basalt (up to several millimeters) and the resulting smaller surface area exposed to the acidic CO_2-rich fluid.

From EPMA elemental mapping results shown in Figure 9, the surroundings and bottom of the pit, previously belonging to clinopyroxene, were confirmed to be smectite with Mg and Si as the main components. The disappearance of clinopyroxene in the basalt block may be attributed to the dissolution of the surrounding smectite. Therefore, the dissolution of smectite may dominate the dissolution of altered basalt in the reservoir upon the injection of CO_2 gas, releasing Mg as one of the main cations into the brine for carbonation. The dissolution of smectite also leads to the stripping of clinopyroxenes, but owing to the relatively large size of the

https://doi.org/10.1021/acsomega.3c06899
ACS Omega 2024, 9, 4429−4438

clinopyroxene particles and the presence of Ca in the brine, the increase in Ca concentration is relatively slow.

3.5. Implications of Developing Effective CO_2 Mineralization Strategies. CO_2 mineralization using more readily available altered basalts is an attractive strategy; however, its feasibility remains unclear. This study evaluated the reactivity of altered basalt by comparing it with unaltered basalt through hydrothermal batch experiments in an acid CO_2-saturated environment at 100 °C. Experiments using basalt powders demonstrated that although the leaching rates of elements from altered basalt were generally an order of magnitude lower than from unaltered basalt, upon injection of CO_2 gas into altered basalt reservoirs, the release of Mg was expected to be rapid (comparable to that of unaltered basalt) due to the fast dissolution of smectite. The dissolution of smectite also resulted in stripping adjacent minerals, typically clinopyroxenes, which could potentially increase their exposure surfaces for reacting with the CO_2-rich fluid. The dissolution of smectite is also expected to enlarge the space for CO_2 storage. However, more research, such as flow-through experiments, is needed to verify the effectiveness of using altered basaltic reservoirs for CO_2 storage.

Several potential challenges in using altered basaltic reservoirs for CO_2 storage were also identified in this study. First, despite the relative reactivity of Ca-bearing minerals, such as clinopyroxene (Figure 4), because of their large particle sizes in basalt, leaching of Ca may be slow. Furthermore, lowering the liquid pH by increasing the CO_2 injection pressure or using an acidic liquid for injection or applying rock fracturing or crushing technologies to increase the exposed surface area (Figure 8) may enhance pyroxene dissolution.

Furthermore, the groundwater in the potential CO_2 storage site usually contains significant amounts of divalent cations, which potentially impedes the leaching of more cations from rocks due to the dissolution/precipitation equilibrium. To overcome these challenges and vary the dissolution/precipitation equilibrium, recent studies, including our previous work, have demonstrated that the incorporation of additives, such as chelating agents, can effectively enhance mineral dissolution by selectively extracting metals.[44,45] The utilization of such advanced approaches should also be considered for the advancement of the CO_2 mineralization technology.

When reacting altered basalt powders with CO_2-saturated brine in this study, Ca and Fe carbonates covered by amorphous SiO_2 were generated during the 360 h reaction, which may represent the initial stage of CO_2 mineralization after the injection of CO_2 into a basalt reservoir. The presence of amorphous SiO_2 coating, which has a low solubility in acidic to neutral environments, is supposed to inhibit the dissolution of carbonates and potentially increase the CO_2 storage capacity. Further investigations are also needed to gain a comprehensive understanding of the carbonation processes occurring in altered basalt reservoirs.

4. CONCLUSIONS

To assess the feasibility of using altered basalt for CO_2 mineralization, this study compared the dissolution behavior of altered and unaltered basalt obtained from an oilfield in the Northeast Japan Arc through batch hydrothermal experiments using a brine solution that simulates the reservoir conditions with 5 MPa CO_2 gas at 100 °C. Indeed, the powder results demonstrated the reactivity of basalt rocks. More specifically, although the leaching rates of elements from altered basalt were generally an order of magnitude lower than those from unaltered basalt in CO_2-saturated acidic environments, similar elemental dissolution behavior was observed for the two basalt powders, with the rates of Ca and Mg leaching the highest.

Block experiments were also conducted to simulate a more realistic environment for CO_2 storage. The observed leaching behavior of elements differed from that of the powder experiments, with Mg leaching dominating in altered basalt and simultaneous Ca and Mg leaching from unaltered basalt. Both powder and block experiments revealed that clay mineral smectite in altered basalt exhibited a rapid and preferred dissolution, providing significant amounts of Mg to the solution for CO_2 mineralization. This suggests an initial Mg-dominated carbonation followed by Ca carbonation when using altered basalt for CO_2 storage. The rapid leaching of Mg also positioned the altered basalt as a promising feedstock for CO_2 mineralization. Future investigations should continue to focus on gaining a comprehensive understanding of the carbonation process occurring in altered basalt with respect to reaction time.

AUTHOR INFORMATION

Corresponding Authors

Jiajie Wang − *Department of Environmental Studies for Advanced Society, Graduate School of Environmental Studies, Tohoku University, Sendai 980-0845, Japan*; orcid.org/0000-0003-0469-5500; Email: wang.jiajie.e4@tohoku.ac.jp

Noriaki Watanabe − *Department of Environmental Studies for Advanced Society, Graduate School of Environmental Studies, Tohoku University, Sendai 980-0845, Japan*; Email: noriaki.watanabe.e6@tohoku.ac.jp

Authors

Masahiko Yagi − *Japan Petroleum Exploration Co., Ltd., Research Center, Chiba 261-0025, Japan*

Tetsuya Tamagawa − *Japan Petroleum Exploration Co., Ltd., Research Center, Chiba 261-0025, Japan*

Hitomi Hirano − *Japan Petroleum Exploration Co., Ltd., Research Center, Chiba 261-0025, Japan*

Complete contact information is available at: https://pubs.acs.org/10.1021/acsomega.3c06899

Notes

The authors declare no competing financial interest.

ACKNOWLEDGMENTS

This study was partially supported by the Japan Society for the Promotion of Science (JSPS) through Grants-in-Aid for Scientific Research (B) (no. 22H02015), Challenging Research (Pioneering) (no. 21K18200), Early-Career Scientists (no. 21K14571), Scientific Research (S) (no. 22H04932), and Japan Petroleum Exploration Co., Ltd., through a joint research project. We thank the Japan Petroleum Exploration Co., Ltd. for allowing us to publish the data in this paper. We also thank Masanobu Kamitakahara at the Graduate School of Environmental Studies, Tohoku University, for helping in the SSA_{BET} analysis.

REFERENCES

(1) Gislason, S. R.; Oelkers, E. H. Geochemistry. Carbon storage in basalt. *Science* **2014**, *344*, 373−374.

https://doi.org/10.1021/acsomega.3c06899
ACS Omega 2024, 9, 4429−4438

(2) Sanna, A.; Uibu, M.; Caramanna, G.; Kuusik, R.; Maroto-Valer, M. M. A review of mineral carbonation technologies to sequester CO2. *Chem. Soc. Rev.* **2014**, *43*, 8049−8080.
(3) Xiong, W.; Wells, R. K.; Menefee, A. H.; Skemer, P.; Ellis, B. R.; Giammar, D. E. CO2 mineral trapping in fractured basalt. *Int. J. Greenhouse Gas Control* **2017**, *66*, 204−217.
(4) Okoko, G. O.; Olaka, L. A. Can East African rift basalts sequester CO2? Case study of the Kenya rift. *Sci. Afr.* **2021**, *13*, No. e00924.
(5) Snæbjörnsdóttir, S. Ó.; Sigfússon, B.; Marieni, C.; Goldberg, D.; Gislason, S. R.; Oelkers, E. H. Carbon dioxide storage through mineral carbonation. *Nat. Rev. Earth Environ.* **2020**, *1*, 90−102.
(6) Snæbjörnsdóttir, S. Ó.; Wiese, F.; Fridriksson, T.; Ármansson, H.; Einarsson, G. M.; Gislason, S. R. CO2 storage potential of basaltic rocks in Iceland and the oceanic ridges. *Energy Procedia* **2014**, *63*, 4585−4600.
(7) Welsby, D.; Price, J.; Pye, S.; Ekins, P. Unextractable fossil fuels in a 1.5°C world. *Nature* **2021**, *597*, 230−234.
(8) Kikuchi, S.; Wang, J.; Dandar, O.; Uno, M.; Watanabe, N.; Hirano, N.; Tsuchiya, N. NaHCO3 as a carrier of CO2 and its enhancement effect on mineralization during hydrothermal alteration of basalt. *Front. Environ. Sci.* **2023**, *11*, No. 1138007.
(9) Galeczka, I.; Wolff-Boenisch, D.; Oelkers, E. H.; Gislason, S. R. An experimental study of basaltic glass−H2O−CO2 interaction at 22 and 50°C: implications for subsurface storage of CO2. *Geochim. Cosmochim. Acta* **2014**, *126*, 123−145.
(10) Gysi, A. P.; Stefánsson, A. Mineralogical aspects of CO2 sequestration during hydrothermal basalt alteration — an experimental study at 75 to 250°C and elevated pCO_2. *Chem. Geol.* **2012**, *306*−*307*, 146−159.
(11) Matter, J. M.; Stute, M.; Snaebjornsdottir, S. O.; Oelkers, E. H.; Gislason, S. R.; Aradottir, E. S.; Sigfusson, B.; Gunnarsson, I.; Sigurdardottir, H.; Gunnlaugsson, E.; Axelsson, G.; Alfredsson, H. A.; Wolff-Boenisch, D.; Mesfin, K.; Taya, D. F. d. l. R.; Hall, J.; Dideriksen, K.; Broecker, W. S. Rapid carbon mineralization for permanent disposal of anthropogenic carbon dioxide emissions. *Science* **2016**, *352*, 1312−1314.
(12) Xing, T.; Ghaffari, H. O.; Mok, U.; Pec, M. Creep of CarbFix basalt: influence of rock−fluid interaction. *Solid Earth* **2022**, *13*, 137−160.
(13) Liu, D.; Agarwal, R.; Li, Y.; Yang, S. Reactive transport modeling of mineral carbonation in unaltered and altered basalts during CO2 sequestration. *Int. J. Greenhouse Gas Control* **2019**, *85*, 109−120.
(14) Wang, J.; Watanabe, N.; Okamoto, A.; Nakamura, K.; Komai, T. Enhanced hydrogen production with carbon storage by olivine alteration in CO2-rich hydrothermal environments. *J. CO2 Util.* **2019**, *30*, 205−213.
(15) Delerce, S.; Bénézeth, P.; Schott, J.; Oelkers, E. H. The dissolution rates of naturally altered basalts at pH 3 and 120 °C: implications for the in-situ mineralization of CO2 injected into the subsurface. *Chem. Geol.* **2023**, *621*, No. 121353.
(16) Wu, J.; Liu, Z.; Yu, X. Plagioclase-regulated hydrothermal alteration of basaltic rocks with implications for the South China Sea rifting. *Chem. Geol.* **2021**, *585*, No. 120569.
(17) Mitsuhata, Y.; Matsuo, K.; Minegishi, M. Magnetotelluric survey for exploration of a volcanic-rock reservoir in the Yurihara oil and gas field. *Japan. Geophys. Prospect.* **1999**, *47*, 195−218.
(18) Yagi, M. Regional metamorphism and hydrothermal alteration related to Miocene submarine volcanism ('green tuff') in the Yurihara oil and gas field, northwest Honshu Island. *Japan. Isl. Arc* **1993**, *2*, 240−261.
(19) Yagi, M.; Ohguch, T.; Akiba, F.; Yoshida, T.; Tiba, T. The Fukuyama volcanic rocks: submarine composite volcano in the Late Miocene to Early Pliocene Akita−Yamagata back-arc basin, northeast Honshu, Japan. *Sediment. Geol.* **2009**, *220*, 243−255.
(20) Humphris, S. E.; Thompson, G. Hydrothermal alteration of oceanic basalts by seawater. *Geochim. Cosmochim. Acta* **1978**, *42*, 107−125.
(21) Raza, A.; Glatz, G.; Gholami, R.; Mahmoud, M.; Alafnan, S. Carbon mineralization and geological storage of CO2 in basalt: mechanisms and technical challenges. *Earth Sci. Rev.* **2022**, *229*, No. 104036.
(22) Black, J. R.; Carroll, S. A.; Haese, R. R. Rates of mineral dissolution under CO2 storage conditions. *Chem. Geol.* **2015**, *399*, 134−144.
(23) Phukan, M.; Vu, H. P.; Haese, R. R. Mineral dissolution and precipitation reactions and their net balance controlled by mineral surface area: an experimental study on the interactions between continental flood basalts and CO2-saturated water at 80 bar and 60 °C. *Chem. Geol.* **2021**, *559*, No. 119909.
(24) Brantley, S. L. Kinetics of mineral dissolution. In *Kinetics of Water-Rock Interaction*; Brantley, S. L.; Kubicki, J. D.; White, A. F., Eds.; Springer: New York, NY, 2008; pp 151−210. DOI: 10.1007/978-0-387-73563-4_5.
(25) Gudbrandsson, S.; Wolff-Boenisch, D.; Gislason, S. R.; Oelkers, E. H. An experimental study of crystalline basalt dissolution from 2 ⩽ pH ⩽ 11 and temperatures from 5 to 75 °C. *Geochim. Cosmochim. Acta* **2011**, *75*, 5496−5509.
(26) Pratt, C.; Kingston, K.; Laycock, B.; Levett, I.; Pratt, S. Geo-Agriculture: Reviewing opportunities through which the geosphere can help address emerging crop production challenges. *Agronomy* **2020**, *10*, 971.
(27) Midttomme, K.; Roaldset, E. The effect of grain size on thermal conductivity of quartz sands and silts. *Pet. Geosci.* **1998**, *4*, 165−172.
(28) Mottl, M. J.; Holland, H. D. Chemical exchange during hydrothermal alteration of basalt by seawater—I. Experimental results for major and minor components of seawater. *Geochim. Cosmochim. Acta* **1978**, *42*, 1103−1115.
(29) Koukouzas, N.; Koutsovitis, P.; Tyrologou, P.; Karkalis, C.; Arvanitis, A. Potential for mineral carbonation of CO2 in Pleistocene basaltic rocks in Volos region (central Greece). *Minerals* **2019**, *9*, 627.
(30) Pogge von Strandmann, P. A. E.; Burton, K. W.; Snæbjörnsdóttir, S. O.; Sigfússon, B.; Aradóttir, E. S.; Gunnarsson, I.; Alfredsson, H. A.; Mesfin, K. G.; Oelkers, E. H.; Gislason, S. R. Rapid CO2 mineralisation into calcite at the CarbFix storage site quantified using calcium isotopes. *Nat. Commun.* **2019**, *10*, 1983.
(31) Shao, H.; Ray, J. R.; Jun, Y.-S. Dissolution and Precipitation of clay minerals under geologic CO2 sequestration conditions: CO2−brine−phlogopite interactions. *Environ. Sci. Technol.* **2010**, *44*, 5999−6005.
(32) Liu, D.; Agarwal, R.; Liu, F.; Yang, S.; Li, Y. Modeling and assessment of CO2 geological storage in the Eastern Deccan Basalt of India. *Environ. Sci. Pollut. Res. Int.* **2022**, *29*, 85465−85481.
(33) Luhmann, A. J.; Tutolo, B. M.; Tan, C.; Moskowitz, B. M.; Saar, M. O.; Seyfried, W. E. Whole rock basalt alteration from CO2-rich brine during flow-through experiments at 150 °C and 150 bar. *Chem. Geol.* **2017**, *453*, 92−110.
(34) Zhang, R.; Zhang, X.; Hu, S. Basalt−water interactions at high temperatures: 1. Dissolution kinetic experiments of basalt in water and NaCl-H2O at temperatures up to 400°C, 23 MPa and implications. *J. Asian Earth Sci.* **2015**, *110*, 189−200.
(35) Tutolo, B. M.; Awolayo, A.; Brown, C. Alkalinity generation constraints on basalt carbonation for carbon dioxide removal at the gigaton-per-year scale. *Environ. Sci. Technol.* **2021**, *55*, 11906−11915.
(36) Huzioka, K. The studies on Green Tuff. *Kagaku* **1956**, *26*, 440−446.
(37) Bern, C. R.; Birdwell, J. E.; Jubb, A. M. Water−rock interaction and the concentrations of major, trace, and rare earth elements in hydrocarbon-associated produced waters of the United States. *Environ. Sci. Process. Impacts* **2021**, *23*, 1198−1219.
(38) Duan, Z.; Sun, R.; Zhu, C.; Chou, I.-M. An improved model for the calculation of CO2 solubility in aqueous solutions containing Na +, K+, Ca2+, Mg2+, Cl−, and SO42−. *Mar. Chem.* **2006**, *98*, 131−139.
(39) Rinder, T.; von Hagke, C. The influence of particle size on the potential of enhanced basalt weathering for carbon dioxide removal -

https://doi.org/10.1021/acsomega.3c06899
ACS Omega 2024, 9, 4429−4438

Insights from a regional assessment. *J. Cleaner Prod.* **2021**, *315*, No. 128178.
(40) Akula, P.; Little, D.; Schwab, P. Thermodynamic evaluation of smectite treated with hydrogen ion stabilizer. *J. Mater. Civ. Eng.* **2020**, *32*, No. 04020098.
(41) Rodriguez-Blanco, J. D.; Shaw, S.; Benning, L. G. The kinetics and mechanisms of amorphous calcium carbonate (ACC) crystallization to calcite, via vaterite. *Nanoscale* **2011**, *3*, 265−271.
(42) Köck, E.; Kogler, M.; Bielz, T.; Klötzer, B.; Penner, S. In situ FT-IR spectroscopic study of CO_2 and CO adsorption on Y_2O_3, ZrO_2, and Yttria-stabilized ZrO2. *J. Phys. Chem. C* **2013**, *117*, 17666−17673.
(43) Kellermeier, M.; Melero-García, E.; Glaab, F.; Klein, R.; Drechsler, M.; Rachel, R.; García-Ruiz, J. M.; Kunz, W. Stabilization of amorphous calcium carbonate in inorganic silica-rich environments. *J. Am. Chem. Soc.* **2010**, *132*, 17859−17866.
(44) Takahashi, R.; Wang, J.; Watanabe, N. Process and optimum pH for permeability enhancement of fractured granite through selective mineral dissolution by chelating agent flooding. *Geothermics* **2023**, *109*, No. 102646.
(45) Watanabe, N.; Takahashi, K.; Takahashi, R.; Nakamura, K.; Kumano, Y.; Akaku, K.; Tamagawa, T.; Komai, T. Novel Chemical stimulation for geothermal reservoirs by chelating agent driven selective mineral dissolution in fractured rocks. *Sci. Rep.* **2021**, *11*, 19994.

https://doi.org/10.1021/acsomega.3c06899
ACS Omega 2024, 9, 4429−4438